Growth Kinetics of ZnO Nanocrystals: A Few Surprises

Ranjani Viswanatha,[†] Heinz Amenitsch,[‡] and D. D. Sarma*,[†,§,‖]

Contribution from the Solid State and Structural Chemistry Unit, Indian Institute of Science, Bangalore 560012, India, Institut of Biophysics and Nanosystems Research, Austrian Academy of Sciences, Schmiedlstr. 6, 8042, Graz, Austria, and Centre for Advanced Materials, Indian Association for the Cultivation of Science, Kolkata 700032, India

Received November 15, 2006; E-mail: mlsdds@iacs.res.in

Abstract: Using extensive state-of-the-art experiments over a wide range of synthesis parameters, such as the temperature and concentrations of different reactants, we establish qualitatively different growth kinetics for ZnO nanocrystals compared to all growth kinetics of semiconductor nanocrystals, including ZnO, discussed so far in the literature. The growth rate is shown to be strongly dependent on the concentration of $(OH)^-$ in an intriguing nonmonotonic manner as well as on temperature and is almost invariably much slower than well-known and generally accepted growth mechanisms based on a diffusion-controlled Ostwald ripening process or that expected in the surface reaction controlled regime. We show that these *qualitatively* different results arise from the unexpected role played by a part of the reactants by inhibiting rather than facilitating the reaction; we explain this extraordinary result in terms of an effective passivating layer around the growing nanocrystals formed by a virtual capping shell of Na^+ ions.

Introduction

Over the past decade, dramatic progress has been made in the synthesis of semiconductor quantum dots using colloidal chemistry techniques. The solution route is one of the most flexible and hence the preferred route of synthesis of semiconducting nanocrystals.[1−5] These recent advances in a wide range of synthesis of nanocrystals from solution-phase reactions should in principle provide a natural testing ground for investigating growth kinetics in the extremely early phases of growth, inaccessible in the past. This has motivated several groups to probe nanocrystal growth in the ultrasmall size regime (see for example refs 2, 6). However it is interesting to note that studies of growth of semiconductor nanocrystals in the quantum confinement regime are relatively few,[6−16] when compared to

the extraordinary rapid increase in investigations reporting synthesis and diverse properties of such systems or compared even to the obvious importance of the field. While the success of these synthesis techniques is indisputable, from a fundamental viewpoint, we still lack a detailed understanding of the processes controlling the growth of crystalline quantum dots in many cases. The primary hindrance to such investigations has been the absence of appropriate techniques to probe the *in situ* growth of nanocrystals. While TEM is the most direct probe to observe the size, morphology, and the size distribution of any assembly of nanocrystals, it is evidently not possible to carry out an *in situ* measurement using TEM under the reaction conditions. *Ex situ* measurements necessarily imply large time steps. Additionally, the sampling size in TEM investigation can at best include only a few hundred of individual nanocrystals, making statistical averaging or determination of the distribution function less certain. Finally TEM often has intrinsic limitations when the nanocrystals tend to agglomerate on the grid or present a low contrast making determination of the size of individual particles with sufficient accuracy difficult, if not impossible. In contrast to the direct probe of the size via TEM investigations, nanocrystal sizes can also be determined using simpler but more indirect methods, for example, by measuring the shifts in absorption or emission energies compared to that for the bulk samples. Indeed, the shift in the emission spectra has been used extensively to understand the growth, for example, in the case of CdSe nanocrystals.[2,3,6] Unfortunately, the emission spectrum

[†] Solid State and Structural Chemistry Unit, Indian Institute of Science.

[‡] Austrian Academy of Sciences.

[§] Indian Association for the Cultivation of Science.

[‖] Also at Jawaharlal Nehru Centre for Advanced Scientific Research, Bangalore 560054, India.

(1) (a) Steigerwald, M. L.; Brus, L. E. *Acc. Chem. Res.* **1990**, *23*, 183. (b) Murray, C. B.; Kagan, C. R.; Bawendi, M. G. *Annu. Rev. Mater. Sci.* **2000**, *30*, 545.

(2) Peng, X.; Wickham, J.; Alivisatos, A. P. *J. Am. Chem. Soc.* **1998**, *120*, 5343.

(3) Yu, W. W.; Peng, X. *Angew. Chem., Int. Ed.* **2002**, *41*, 2368.

(4) Nanda, J.; Sapra, S.; Sarma, D. D.; Chandrasekharan, N.; Hodes, G. *Chem. Mater.* **2000**, *12*, 1018.

(5) Viswanatha, R.; Sapra, S.; Sen Gupta, S.; Satpati, B.; Satyam, P. V.; Dev, B. N.; Sarma, D. D. *J. Phys. Chem. B* **2004**, *108*, 6303.

(6) Qu, L.; Yu, W. W.; Peng, X. *Nanolett.* **2004**, *4*, 465.

(7) Barglik-Chory, C.; Münster, A. F.; Strohm, H.; Remenyi, C.; Müller, G. *Chem. Phys. Lett.* **2003**, *374*, 319.

(8) Peng, Z. A.; Peng, X. *J. Am. Chem. Soc.* **2002**, *124*, 3343.

(9) Qu, L.; Peng, X. *J. Am. Chem. Soc.* **2002**, *124*, 2049.

(10) Bullen, C. R.; Mulvaney, P. *Nano Lett.* **2004**, *4*, 2303.

(11) Dai, Q.; Li, D.; Chen, H.; Kan, S.; Li, H.; Gao, S.; Hou, Y.; Liu, B.; Zou, G. *J. Phys. Chem. B* **2006**, *110*, 16508.

(12) Peng, Z. A.; Peng, X. *J. Am. Chem. Soc.* **2001**, *123*, 1389.

(13) Thoma, S. G.; Sanchez, A.; Provencio, P. P.; Abrams, B. L.; Wilcoxon, J. P. *J. Am. Chem. Soc.* **2005**, *127*, 7611.

(14) Talapin, D. V.; Rogach, A. L.; Shevchenko, E. V.; Kornowski, A.; Haase, M.; Weller, H. *J. Am. Chem. Soc.* **2002**, *124*, 5782.

(15) Pesika, N. S.; Hu, Z.; Stebe, K. J.; Searson, P. C. *J. Phys. Chem. B* **2002**, *106*, 6985.

(16) Wong, E. M.; Hoertz, P. G.; Liang, C. J.; Shi, B.; Meyer, G. J.; Searson, P. C. *Langmuir* **2001**, *17*, 8362.

of most wide band gap semiconductor nanocrystals, like ZnS,[17] is dominated by surface state emissions; such an emission wavelength is generally broad and governed by the details of the surface states rather than by the size of the nanocrystals. Therefore, in most cases, the emission spectrum is not suitable even as an indirect probe of the size. However, the UV-absorption spectra are relatively insensitive to the presence of surface states. Therefore, it is better suited to study the growth of nanocrystals. In this context, we note that the size of the nanocrystals is determined from the shift in the absorption edge using theoretical models and hence the size obtained is highly dependent on the accuracy of the theoretical models employed. Moreover, the size dependence of absorption and emission spectra becomes quite insensitive beyond the excitonic diameter. Hence, these techniques cannot be used for the later stages of the growth. The technique that is most suited to determine the *in situ* size and size distribution of nanocrystals during the growth process is small-angle X-ray scattering (SAXS) measurements. This offers a direct probe, since the scattering cross section depends directly on the shape and size of the nanocrystal. Unlike in the case of absorption or emission energy shifts, where the size of the nanocrystal is indirectly involved via the change in the electronic structure with the size in the quantum confinement regime, the X-ray scattering function is directly controlled by only the shape and size of nanocrystals. The major drawback of SAXS is the low scattering cross section leading to a poor signal-to-noise ratio in all but highly concentrated cases. This can be partly offset by the use of an exceedingly brilliant source such as a synchrotron source; however, even in such cases, the low concentration limit often encountered in a typical synthesis condition remains below the sensitivity limit of SAXS. Hence, it is essential to study the growth of nanocrystals using a combination of techniques, thus validating the sizes determined by various methods in the concentration and size regime where the different techniques have overlapping applicability and using one of the techniques when the other is inaccessible in the regime of interest.

Additionally, the scarcity of literature reports on the growth of nanocrystals may also presumably be due to the belief that the growth of nanocrystals occurs via the Ostwald ripening behavior, though extensive experimental verification in different systems has been absent. Recent theoretical investigations[18] on the growth of nanocrystals, however, suggest that the growth could be either controlled by diffusion of the particles, i.e., Ostwald ripening, or controlled by the reaction at the surface or by both parameters, even in the absence of capping agents. The determination kinetics of growth under the real synthetic conditions is further complicated by the presence of the interactions with the capping agents, which is necessary to control the size and size distribution of the nanocrystals, and is beyond the scope of the Lifshitz, Slyozov, and Wagner (LSW) theory of Ostwald ripening. Several investigations in the literature report the growth of nanocrystals carried out in the presence of capping agents;[2,3,6−16] in these cases, the growth would be a product of several complex processes, though partial signatures of either of the two limiting mechanisms, diffusion or reaction controlled regimes, might be observed. From a fundamental point of view, however, it is clear that the nanocrystal growth in solutions in absence of any capping agent is the most logical ground for critically probing the growth kinetics, as theoretical models and results are available only for this limit.

The growth kinetics of ZnO nanocrystals is one of the earliest[19] studied among the semiconductor nanocrystals as well as extensively studied in the absence of capping agents with systematic variations in various control parameters, such as the concentration of the reactants, nature of the solvent, and the reaction temperature, invariably arriving at the conclusion that the growth of ZnO nanocrystals follows the diffusion-limited ripening process.[20−24] The growth in all these cases was probed by following the time-evolution of the UV-absorption spectra which were then analyzed in terms of Effective Mass Approximation (EMA), which relates the band gap and the size of the nanocrystals. However, it is well-known that EMA overestimates the size in general for semiconductor nanocrystals;[25−28] such an overestimation has been recently established[29] specifically for the case of ZnO. This makes the conclusions of the previous studies on ZnO growth somewhat uncertain, prompting us to reinvestigate the growth kinetics of this important material.

In this work, we have investigated the growth kinetics of ZnO nanocrystals with a combination of SAXS at a third generation, highly brilliant, synchrotron source and absorption spectroscopy in conjunction with the accurate information of band gap variation with size[29] and size distribution.[30] Our studies point to several unusual features including the observation that the growth of nanocrystals can be strongly hindered by the reactant itself. This has further consequences, leading to a growth kinetics for ZnO nanocrystals that has a *qualitatively* different growth model compared to what has been discussed so far in the literature including the nearly universally accepted diffusion-limited Ostwald ripening process.

Experimental Section

ZnO nanocrystals were synthesized using zinc acetate and sodium hydroxide in isopropanol. A typical synthesis involves dissolving the required amount of zinc acetate in 42 mL of isopropanol with constant stirring at 50 °C and then quenching in ice. To this solution, the required concentration of NaOH in 8 mL of isopropanol is suddenly injected, and the solution is maintained at various temperatures in a water bath. UV-absorption spectra of the reaction mixture were recorded at various times using a Perkin-Elmer double beam LM-35 spectrophotometer. Pure isopropanol (*i*-PrOH) was used as the reference blank solution for the samples. *In situ* SAXS measurements were recorded using an image plate detector, Mar180 (MarResearch, Hamburg, Germany), at

(17) Sapra, S.; Nanda, J.; Anand, A.; Bhat, S. V.; Sarma, D. D. *J. Nanosci. Nanotechnol.* **2003**, *3*, 392.
(18) Talapin, D. V.; Rogach, A. L.; Haase, M.; Weller, H. *J. Phys. Chem. B* **2001**, *105*, 12278.
(19) Wong, E. M.; Bonewich, J. E.; Searson, P. C. *J. Phys. Chem. B* **1998**, *102*, 7770.
(20) Hu, Z.; Escamilla Ramirez, D. J.; Heredia Cervera, B. E.; Oskam, G.; Searson, P. C. *J. Phys. Chem. B* **2005**, *109*, 11209.
(21) Pesika, N. S.; Stebe, K. J.; Searson, P. C. *J. Phys. Chem. B* **2003**, *107*, 10412.
(22) Pesika, N. S.; Hu, Z.; Stebe, K. J.; Searson, P. C. *J. Phys. Chem. B* **2002**, *106*, 6985.
(23) Hu, Z.; Oskam, G.; Searson, P. C. *J. Colloid Interface Sci.* **2003**, *263*, 454.
(24) Oskam, G.; Hu, Z.; Penn, R. L.; Pesika, N.; Searson, P. C. *Phys. Rev. E* **2002**, *66*, 11403.
(25) Lippens, P. E.; Lannoo, M. *Phys. Rev. B* **1989**, *39*, 10935.
(26) Sapra, S.; Shanti, N.; Sarma, D. D. *Phys. Rev. B* **2002**, *66*, 205202.
(27) Sapra, S.; Sarma, D. D. *Phys. Rev. B* **2004**, *69*, 125304.
(28) Viswanatha, R.; Sapra, S.; Saha-Dasgupta, T.; Sarma, D. D. *Phys. Rev. B* **2005**, *72*, 045333.
(29) Viswanatha, R.; Sapra, S.; Satpati, B.; Satyam, P. V.; Dev, B. N.; Sarma, D. D. *J. Mater. Chem.* **2004**, *14*, 661.
(30) Viswanatha, R.; Sarma, D. D. *Chem.−Eur. J.* **2006**, *12*, 180.
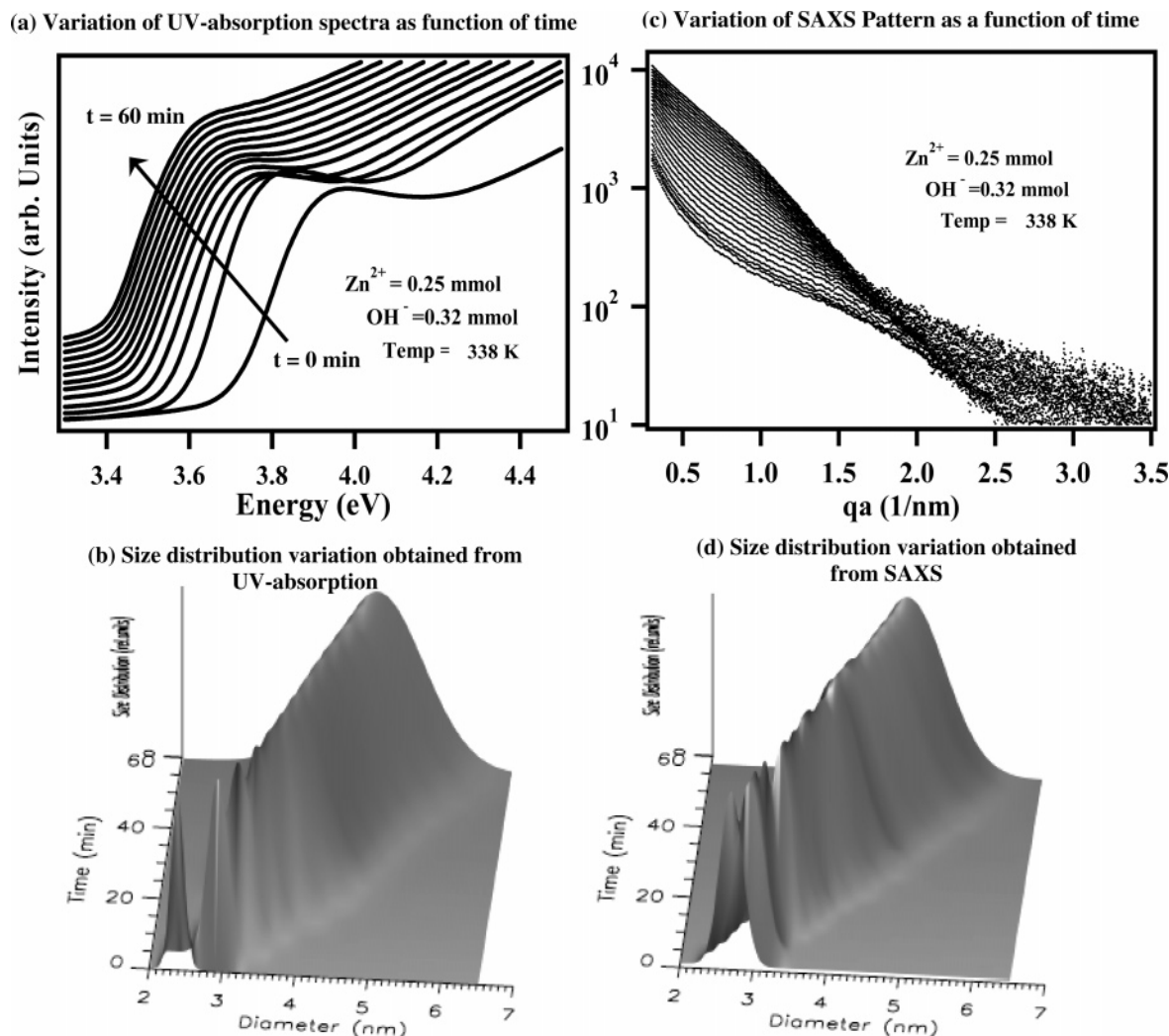
Figure 1. (a) Typical UV-absorption data at a temperature of 338 K obtained after different time intervals. (b) Typical time evolution variation of the diameter and the distribution of diameters of ZnO nanocrystals obtained from the analysis of the UV-absorption data shown in part a. (c) Typical variation of the SAXS patterns as a function of time for a given concentration of NaOH at 338 K. (d) Typical time evolution variation of the diameter and the distribution of diameters of ZnO nanocrystals obtained from the analysis of the SAXS data shown in part c.

the Austrian SAXS beamline[31] at the Italian synchrotron center, ELETTRA, Trieste, operated at 2 GeV. The beamline was set to a camera length of 1.65 m and an X-ray energy of 16 keV. Silver behenate $(CH_3(CH_2)_{20}\text{-}COOAg)$, with a *d*-spacing of 58.38 Å,[32] was used as a standard to calibrate the angular scale of the 2-D detector. SAXS of pure *i*-PrOH was used as the background. The reaction solution was circulated in a 2 mm quartz capillary using a flow through technique[33] to avoid deposition of the particles on the walls of the capillary. The reaction mixture was kept at a constant temperature using an oil bath and a KHR sample stage (Anton Paar, Graz, Austria). Since the SAXS data were analyzed assuming spherical nanocrystals, this assumption was explicitly verified by carrying out transmission electron microscopic investigations at several points of the growth process under different conditions. Such studies were carried out using a Technai F30 UHR version electron microscope using a Field Emission Gun (FEG) at an accelerating voltage of 300 kV. These studies not only confirmed the spherical shapes of nanocrystals at all stages of our study but also

(31) Amenitsch, H.; Bernstorff, S.; Kriechbaum, M.; Lombardo, D.; Mio, H.; Rappolt, M.; Laggner, P. *J. Appl. Crystallogr.* **1997**, *30*, 872.
(32) Huang, T. C.; Toraya, H.; Blanton, T. N.; Wu, Y. *J. Appl. Crystallogr.* **1993**, *26*, 180.
(33) Agren, P.; Linden, M.; Rosenholm, J. B.; Schwarzenbacher, R.; Kriechbaum, M.; Amenitsch, H.; Laggner, P.; Blanchard, J.; Schuth, F. *J. Phys. Chem. B* **1999**, *103*, 5943.

provided a critical confirmation of size distributions by SAXS at specific points of the growth process.

Results and Discussion

Typical time-resolved *in situ* UV-absorption spectra obtained at given concentrations of NaOH and $Zn(OAc)_2$, 0.32 and 0.25 mmol, respectively, and at a temperature of 338 K are shown as a function of the reaction time in Figure 1a. From the shifting edge of these spectra toward lower energies, it is clear that the size of the nanocrystal increases as a function of time. The average diameter and the size distribution of the nanocrystals were determined[29] from the recent realistic calculations reported in the literature[30] that are known to show good agreement with experimental data over a wide range of sizes. Figure 1b shows the resulting time evolution of the size distribution function of ZnO nanocrystals under these reaction conditions.

Due to the indirect nature of the probe used, we have cross-checked the validity of estimating the size distribution function from UV-absorption spectroscopy, by carrying out time-resolved *in situ* SAXS for several cases with an exposure time of 60 s in order to be able to measure with some reasonable signal-to-

noise ratio. The typical variation of patterns as a function of time is shown in Figure 1c. The changes in SAXS pattern clearly show the growth of the nanocrystal as a function of time. In order to obtain more quantitative information, we have assumed the presence of spherical particles of average diameter d and a Gaussian distribution of sizes with a width of Δd and fitted the data[34] to the spherical form factor using the equation $S(q) = A/q^{(4+\beta)} + B\int D(x/r)\, x^6 F^2(qx)\, dx$. The first term (Porod function) of the equation is due to the background, and the second term, due to the presence of spherical particles. We carried out least squared error fittings of experimental data, and typical fits at a few selected time intervals are shown in the supporting data. The time evolution of the size distribution function determined from such an analysis of the SAXS data is shown in Figure 1d; these are in striking agreement with the size distribution function obtained from UV-absorption analysis (see Figure 1b), validating the present approach. In the main part of this article, we present results derived from absorption spectra, in view of its higher sensitivity to such low concentrations of nanocrystals in comparison to the results of SAXS, leading to results with a considerably better signal-to-noise ratio. However, we provide an extensive comparison between results from the absorption edge and those from SAXS in the Supporting Information to establish the validity of these results beyond any reasonable doubt.

In order to understand the growth kinetics of ZnO nanocrystals, we investigated the temperature dependence of the growth rate by monitoring the average diameter of growing nanocrystals as a function of time at different temperatures for various fixed concentrations of the reactants. A set of typical variations of the diameter as a function of time is shown in Figure 2a for different temperatures. The dependence of the diameter, d, on time, t, in Figure 2a could not be fitted to the well-known expression, $d^3 - d_0^3 = kt$, this form being predicted by the LSW theory[35,36] for diffusion controlled growth processes, suggesting the inapplicability of this standard growth model to the case of ZnO nanocrystals. In order to obtain an empirical, quantitative description, the $d(t)$ data were fitted with the expression $d^x - d_0^x = kt$, where the value of x is allowed to vary to obtain the best fit. It is known that the growth of nanocrystals in the absence of any capping agent should yield an exponent (x) between 2 and 3, 2 being the limiting value where the growth is controlled entirely by the surface reaction and 3 being the limiting value when the growth is solely diffusion limited.[37] The fits obtained from the least-squared-error fitting of the present experimental data to the assumed $d^x - d_0^x = kt$ dependence are shown by the solid lines overlapping the data points in Figure 2a. Interestingly, the value of x obtained from such an analysis of the data in Figure 2a was in the range 4−8, far from the expected values 2 and 3 for the well-known surface-reaction-limited or diffusion-limited processes, respectively. In order to gain further insight into the mechanism of growth that gives rise to such an unusual growth kinetics, we plot the diameter of the growing nanocrystal as a function of time at a fixed temperature of 338 K in Figure 2b for different concentrations of NaOH. It is evident from this figure that the
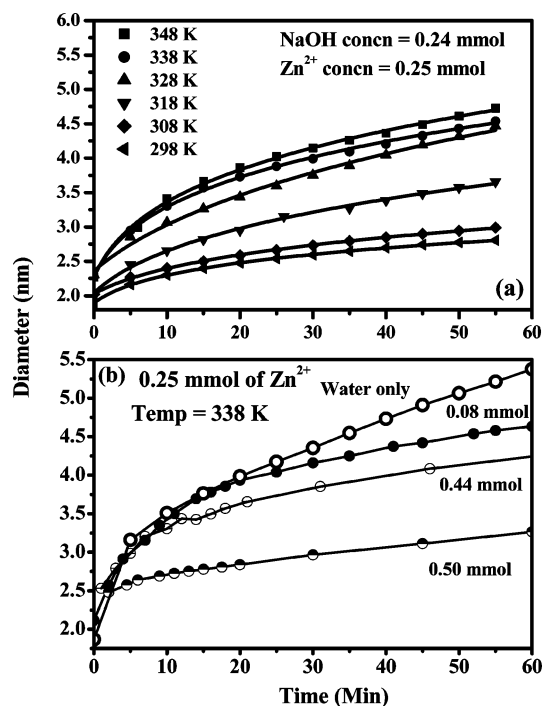

Figure 2. (a) Typical time evolution of the diameter of the nanocrystals for a fixed concentration of NaOH at different temperatures. The solid lines show the fit of the form $d^x - d_0^x = kt$. (b) The variation of the diameter of ZnO nanocrystals as a function of time for different concentrations of NaOH at 338 K. The solid line shows a best fit of the form $d^x - d_0^x = kt$.

size of the growing nanocrystal at any given time depends strongly on the concentration of NaOH. This observation is qualitatively different from the expected behavior within the diffusion-limited Ostwald ripening process, where the diameter of the growing nanocrystal is a function only of time and temperature, but not of the concentration, since the diffusion rate is independent of the reactant concentration in such dilute limits. We observe that the best fits to the form $d^x - d_0^x = kt$, shown with solid lines overlapping the experimental data in Figure 2b, were obtained for the exponent values of 5.7, 6.7, and 7.3 for the three different concentrations of NaOH of 0.08, 0.44, and 0.50 mmol, respectively, and 3.1 for the case of only[37] water.

We have probed the origin of these exotic behaviors by carrying out a large number of studies, systematically varying the reaction conditions, such as the temperature and the concentrations of Zn^{2+} and OH^- ions, over wide ranges. The values of x obtained for reactions carried out at different concentrations of NaOH as a function of temperature are plotted in Figure 3a. Figure 3a makes it evident that x is in general far from the expected[37] range (2−3). Further, it can be seen that x decreases gradually with increasing temperature and approaches the value of 3, expected for the diffusion-limited process and marked by a dashed line in the figure. The considerably larger x value clearly suggests that the growth of ZnO nanocrystals is much slower than the usual and expected rate of growth. Interestingly, we find that the growth rate is consistently slower, as evidenced by a larger x value, with increasing NaOH concentration. Since it is known[38] that the formation of ZnO is hindered in the presence of a high pH (>10) in aqueous solutions, we measured the pH of the reaction mixtures and

(34) Beaucage, G. *J. Appl. Crystallogr.* **1995**, *28*, 717.
(35) Lifshitz, I. M.; Slyozov, V. V. *J. Phys. Chem. Solids* **1961**, *19*, 35.
(36) Wagner, C. *Z. Elektrochem.* **1961**, *65*, 581.
(37) Viswanatha, R.; Santra, P. K.; Das Gupta, C.; Sarma, D. D. Unpublished results.

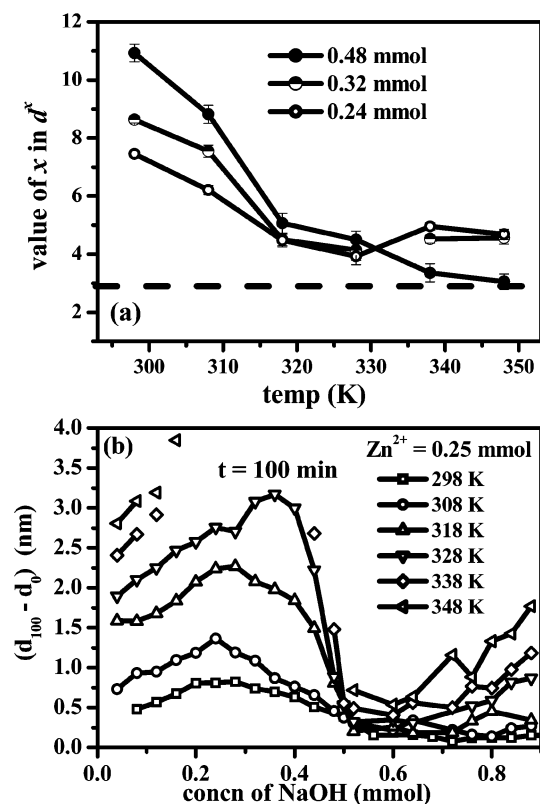(38) Degen, A.; Kosec, M. *J. Eur. Cer. Soc.* **2000**, *20*, 667.

Figure 3. (a) Variation of the value of x in the above equation as a function of temperature for various concentrations of NaOH. (b) Variation of the difference in diameter ($d_{100} - d_0$) of ZnO nanocrystals as a function of concentration of NaOH for different synthesis temperatures.

found pH values ranging between 7 and 8.5 in every case, consistent with low concentrations of NaOH used in these reactions. Additionally, we observe that the formation of ZnO in all our reactions is instantaneous and only the growth of the cluster size is hindered by the presence of NaOH. Such a behavior is unusual, since one would not normally expect the growth process to proceed slower in the presence of more reactants. Since even a small amount of water is known[5] to influence, specifically increase, the growth rate of ZnO nanocrystals, it is necessary to exclude the possibility of a trace amount of water present in the form of water absorbed due to the hygroscopic nature of NaOH as well as the water of hydration in zinc acetate being responsible for such nonmonotonic growth behaviors. So we carried out the same reactions in the presence of anhydrous silica gel to absorb any water that may be present in the reaction mixture; we also carried out such reactions with the deliberate addition of small quantities of water for different concentrations of NaOH. Though the growth rate was expectedly found to depend quantitatively on the extent of trace water in the reaction mixture, all qualitative features, such as the nonmonotonocity of the growth with NaOH concentration, were found to be independent of the water content in these experiments. So, the only way one can understand these results is to anticipate that the growth of ZnO nanocrystals is hindered in the presence of the base by some mechanism that is dependent on the concentration of the base.

In order to understand the exact dependence on the concentration of the base, we carried out reactions at different temperatures and base concentrations. A typical set of data is shown in Figure 3b, illustrating the variation in the diameter

after a fixed time of 100 min, i.e., $d_{100} - d_0$, for a fixed concentration of Zn(OAc)$_2$ as a function of NaOH concentration at various temperatures; similar dependencies are observed for other fixed times also. Several interesting and puzzling properties are evident in these results. Unlike Figure 3a, with results for few concentrations exhibiting an apparent monotonic decrease in the growth rate in terms of an increasing x with concentration at least at lower temperatures, Figure 3b makes it evident that there is a strong nonmonotonic variation in the growth as a function of base concentration. Thus, we find an initial increase in the size with increasing base concentration up to a maximum base concentration, followed by a rapid decrease and finally a slow increase in the most concentrated regime. Most intriguingly, the increase in the diameter exhibits a precipitous drop to achieve an exceedingly slow growth at 0.5 mmol of NaOH, *irrespective of the temperature of the synthesis*. This suggests that ZnO nanocrystal growth with time is inhibited very strongly at this concentration of NaOH; in fact, the results in Figure 3b suggest a remarkably slow growth of ZnO nanocrystals for NaOH concentrations higher than 0.5 mmol at all temperatures.

The initial increase in the diameter followed by a decrease, eventually leading to almost an absence of growth at higher concentrations of NaOH, as illustrated in Figure 3b, suggests that the observed growth is possibly a result of two competing mechanisms. It is obvious that the growth of ZnO nanocrystals is assisted by the diffusion of reactants. Hence, the results in Figure 3b points to a competing hindering mechanism whose efficacy increases with the concentration of NaOH up to a critical concentration (0.5 mmol in the case of Figure 3b) independent of the temperature. It is important to note here that the growth of ZnO nanocrystals with time is the fastest in the presence of only water (100 mmol) in complete absence of any NaOH, as illustrated for the reaction at 338 K in Figure 2b. We observed the same phenomena at all other temperatures too, indicating that the presence of NaOH, besides providing the hydroxyl ions necessary for the growth of ZnO nanocrystals, also leads to another process that impedes the growth of the nanocrystals. Here we note that the NaOH not only is a source of hydroxyl ions to act as a reactant forming Zn(OH)$_2$ that dissociates to form ZnO and water but also provides the counterion, Na$^+$. This suggests that either the Na$^+$ ion or the hydroxyl ion could be acting as a capping agent, thus impeding the growth of the nanocrystal. In order to identify the real capping agent, we first used pure water as a source of hydroxyl ions in the complete absence of any sodium ion and carried out similar reactions. Significantly, we observed clearly the formation and growth of ZnO nanocrystals under these conditions with the growth behavior qualitatively different from what has been found here with NaOH; specifically, we do not observe the nonmonotonic dependencies in the absence of Na$^+$ ions, suggesting that the Na$^+$ ion is indeed responsible for these unusual behaviors. In order to further confirm this hypothesis, we carried out a reaction at 318 K with the NaOH concentration of 0.36 mmol. In this reaction we specifically added more sodium ions by the addition of sodium acetate into the solution and found that the growth rate of the nanocrystal is suppressed strongly, though we observed the maximum growth for this concentration of NaOH in the absence of sodium acetate. Thus, these experiments establish that sodium ions indeed act as a
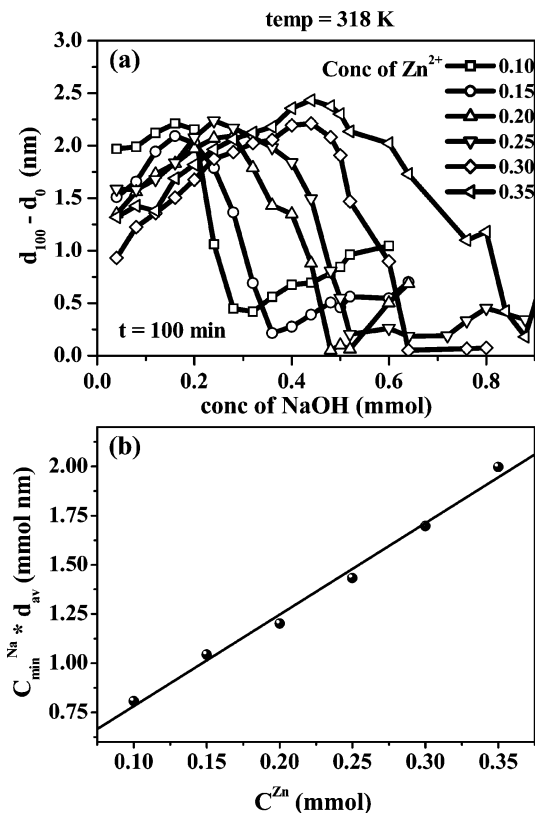
Figure 4. (a) Variation of the difference in diameter ($d_{100} - d_0$) of ZnO nanocrystals as a function of the concentration of NaOH for different Zn^{2+} concentrations. (b) Variation of the product of hydroxyl ion concentration required to obtain zero growth rate and the diameter of the nanocrystal as a function of Zn^{2+} concentration.

capping agent in this reaction. In this context, we note that the Na^+ ion can migrate to the nanocrystal surface. Such a diffusion of Na^+ ions toward the growing nanocrystal surface is definitely helped by the charge on the OH^- ion, as the hydroxyl ion attaches itself to the nanocrystal surface; in other words, it is natural to expect Na^+ ions to diffuse to the growing nanocrystals and act as counterions to the OH^- species attached to the nanocrystal, thereby hindering the approach of Zn^{2+} ions necessary for further growth of the nanocrystal. With increasing NaOH concentration, the Na^+ counterions can provide an increasingly effective shield around the nanocrystal, thereby acting efficiently as a capping agent, inhibiting the growth.

If this mechanism, proposed above, is indeed responsible for the unusual experimental observations, we would expect the concentration of NaOH required to precipitously suppress the growth of the nanocrystal to depend in some unique way on the reaction conditions. Specifically, we note that the proposed scenario of Na^+ ions providing a shell of counterions around each nanocrystal in fact requires a simple relationship between the NaOH concentration, C_{min}^{Na}, corresponding to the minimum growth rate, in other words, optimal capping, and the Zn^{2+}

concentration, C^{Zn}. It is clear that C_{min}^{Na} has to be proportional to the total surface area of all the nanocrystals in the solution in order to provide an effective passivation. If we assume that the nanocrystals have an average radius of R_{av}, the total surface area can be easily shown to be proportional to C^{Zn}/R_{av}. This implies that C_{min}^{Na} should be proportional to C^{Zn}/R_{av}, or in other words $C_{min}^{Na} * R_{av} \propto C^{Zn}$. In order to test the proposed scenario critically, we measured the growth of ZnO nanocrystals as a function of NaOH concentration for different concentrations of Zn^{2+} after a fixed growth time of 100 min and at a growth temperature of 318 K. The results, plotted in Figure 4a, exhibit a strong variation of C_{min}^{Na} as a function of Zn^{2+} concentration. This is in contrast to the striking invariance of this optimal concentration with respect to changes in the reaction temperature for the fixed Zn^{2+} concentration (see Figure 3b). We plot $C_{min}^{Na} * d_{av}$ (where $d_{av} = 2R_{av}$) vs C^{Zn} in Figure 4b, based on the results shown in Figure 4a. The remarkable straight line behavior of the plot undoubtedly establishes the aforementioned proportionality, thereby establishing the mechanism proposed here.

Conclusion

We have studied the growth kinetics of ZnO nanocrystals in the usual synthesis method carried out in the presence of a strong base. In contrast to earlier reports, we find that the growth kinetics differs *qualitatively* from the usually expected diffusion-limited Ostwald ripening mechanism, exhibiting a drastically slower rate of growth and a remarkable nonmonotonic dependence on the concentration of NaOH. Specific experiments establish that such a behavior arises due to the counterions, Na^+, being attracted by the hydroxyl ions around the nanocrystal forming a virtual capping layer. This unexpected twist in chemistry takes this case of nanocrystal growth in the absence of any added capping agent outside the range of applicability of existing theories. These results further lead to a fundamentally new understanding of the growth process of nanocrystals, not realized previously, where the reactant itself provides a passivating effect, and may be useful in designing new strategies for synthesis.

Supporting Information Available: Typical fitting of the SAXS data and a comparison of the diameter as a function of time at different concentrations of NaOH and different temperatures using SAXS and UV-absorption spectroscopy. This material is available free of charge via the Internet at http://pubs.acs.org.

JA068161B